

Cosmic Microwave Background Quadrupole and Ellipsoidal Universe

L. Campanelli^{a,b,1}, P. Cea^{c,d,2}, and L. Tedesco^{c,d,3}

^a*INFN - Sezione di Ferrara, I-44100 Ferrara, Italy,*

^b*Dipartimento di Fisica, Università di Ferrara, I-44100 Ferrara, Italy,*

^c*INFN - Sezione di Bari, I-70126 Bari, Italy,*

^d*Dipartimento di Fisica, Università di Bari, I-70126 Bari, Italy*

Abstract

Recent Wilkinson Microwave Anisotropy Probe (WMAP) data confirm the Cosmic Microwave Background (CMB) quadrupole anomaly. We further elaborate our previous proposal that the quadrupole power can be naturally suppressed in axis-symmetric universes. In particular, we discuss in greater detail the CMB quadrupole anisotropy and considerably improve our analysis. As a result, we obtain tighter constraints on the direction of the axis of symmetry as well as on the eccentricity at decoupling. We find that the quadrupole amplitude can be brought in accordance with observations with an eccentricity at decoupling of about 0.64×10^{-2} . Moreover, our determination of the direction of the symmetry axis is in reasonable agreement with recent statistical analyses of cleaned CMB temperature fluctuation maps obtained by means of improved internal linear combination methods as Galactic foreground subtraction technique.

¹E-mail: campanelli@fe.infn.it

²E-mail: paolo.cea@ba.infn.it

³E-mail: luigi.tedesco@ba.infn.it

1 Introduction

The Cosmic Microwave Background (CMB) has had a profound impact on modern cosmology and greatly improved our understanding of the universe. The CMB angular power spectrum is indeed very sensitive to the origin and evolution of the cosmic density fluctuations.

The temperature fluctuations of CMB are observed at the level of $\Delta T/\langle T \rangle \sim 10^{-5}$ [1]. The high resolution data provided by the Wilkinson Microwave Anisotropy Probe (WMAP) [2, 3, 4, 5] confirmed that the CMB anisotropy data are in striking agreement with the predictions of the simplest inflation model.

However, the 3-years WMAP data (WMAP3) display at large angular scales some anomalous features. The most important discrepancy resides in the low quadrupole moment, which signals an important suppression of power at large scales, although the probability of quadrupole being low is not statistically compelling. The problem consists into the fact that the power of the quadrupole is substantially reduced with respect to the value of the best-fit Λ -dominated cold dark matter (Λ CDM) standard model. If this discrepancy turns out to have a cosmological origin, then it could have far reaching consequences for our understanding of the universe and in particular for the standard inflationary picture. This peculiarity emerged since 1992 when the first data of the differential microwave radiometer (COBE/DMR) appeared [1]. Since then, in 2003 (WMAP) and in 2006 (WMAP3) this behavior was confirmed. In fact, the WMAP3 data give a quadrupole power of $211 \mu\text{K}^2$, while the expected value in Λ -dominated cold dark matter model is about $1252 \mu\text{K}^2$.

In the last years, the “smallness” of CMB quadrupole has been subject to very intensive studies because it may signal a non-trivial topology of the large scale geometry of the universe [6]. Indeed, several possibilities have been advanced in the recent literature to understand the suppression of the quadrupole power [7, 8] (for other large scale anomalies in the angular distribution of CMB see Ref. [9]).

Recently [10] we showed that, allowing the large-scale spatial geometry of our universe to be plane-symmetric with eccentricity at decoupling of order 10^{-2} , the quadrupole amplitude could be drastically reduced without affecting higher multipoles of the angular power spectrum of the temperature anisotropy. Remarkably, the “ellipsoidal” (or “eccentric”) universe has been considered also in non-standard cosmological models, such as braneworld cosmology [11].

There are different mechanisms which could induce a planar symmetry in the spatial geometry of the universe [12]. Among these, the most interesting examples include a cosmic domain wall, a cosmic string and an almost uniform cosmic magnetic field. In particular, the cosmic magnetic field seems to be of relevance since several observations suggest the presence of magnetic fields correlated on cosmic scales [13] (for a recent study of the effects of cosmic magnetic fields on large-scale structures of the universe see Ref. [14], while for influence of cosmic fields on the expansion of the universe see Ref. [15]). There are several possible mechanisms to generate cosmological magnetic fields. For instance, magnetic fields might be produced during [16, 17] or after [18] the inflation era.

In this paper, we further discuss the proposal advanced in Ref. [10] where we showed that cosmic microwave background quadrupole power can be naturally suppressed in plane-symmetric universes. In particular, we discuss in greater detail the CMB quadrupole anisotropy and considerably improve the analysis presented in our previous paper [10]. As a result, we obtain tighter constraints on the direction of the axis of symmetry as well as on the eccentricity at decoupling.

The plan of the paper is as follows. In Sec. 2 we discuss the Einstein's equations for cosmological models with planar geometry, and we describe the mechanisms to generate the eccentricity in the universe expansion by means of magnetic fields, domain walls or cosmic strings; Sec. 3 deals with the analysis of CMB anisotropies including the asymmetric contributions to the temperature anisotropy. In Sec. 4 we discuss the constraints on cosmic magnetic fields arising from primordial nucleosynthesis the large scale structure formation. Finally, we draw our conclusions in Sec. 5. Some technical details are relegated in the Appendix.

2 Cosmological models with planar symmetry

We are interested in cosmological models with planar symmetry. The most general plane-symmetric line element [19] is:

$$ds^2 = dt^2 - a^2(t)(dx^2 + dy^2) - b^2(t) dz^2, \quad (2.1)$$

where a and b are the scale factors. The metric (2.1) corresponds to considering the xy -plane as a symmetry plane.

The non-zero Christoffel symbols corresponding to the metric (2.1) are:

$$\Gamma_{11}^0 = \Gamma_{22}^0 = a\dot{a}, \quad \Gamma_{33}^0 = b\dot{b}, \quad \Gamma_{01}^1 = \Gamma_{02}^2 = \dot{a}/a, \quad \Gamma_{03}^3 = \dot{b}/b, \quad (2.2)$$

where a dot indicates the derivative with respect to the cosmic time. The non-zero Ricci tensor components turn out to be:

$$R_0^0 = -2 \left(\frac{\ddot{a}}{a} + \frac{\ddot{b}}{b} \right), \quad (2.3)$$

$$R_1^1 = R_2^2 = - \left[\frac{\ddot{a}}{a} + \left(\frac{\dot{a}}{a} \right)^2 + \frac{\dot{a}}{a} \frac{\dot{b}}{b} \right], \quad (2.4)$$

$$R_3^3 = - \left(\frac{\ddot{b}}{b} + 2 \frac{\dot{a}}{a} \frac{\dot{b}}{b} \right). \quad (2.5)$$

The most general energy-momentum tensor consistent with planar symmetry is

$$T^\mu_\nu = \text{diag}(\rho, -p_\parallel, -p_\parallel, -p_\perp). \quad (2.6)$$

It can be made up of two different components: an anisotropic contribution,

$$(T_A)^\mu_\nu = \text{diag}(\rho^A, -p_\parallel^A, -p_\parallel^A, -p_\perp^A), \quad (2.7)$$

which induces the planar symmetry –as, for example, a uniform magnetic field, a domain wall, or a cosmic string–, and an isotropic contribution,

$$(T_I)^\mu{}_\nu = \text{diag}(\rho^I, -p^I, -p^I, -p^I), \quad (2.8)$$

such as vacuum energy, radiation, matter, or cosmological constant. Exact solutions of Einstein's equations for different kind of plane-symmetric plus isotropic components can be found in Ref. [12].

Taking into account the above energy-momentum tensors, the Einstein's equations

$$R_{\mu\nu} - \frac{1}{2}g_{\mu\nu}R = 8\pi GT_{\mu\nu}, \quad (2.9)$$

read

$$\left(\frac{\dot{a}}{a}\right)^2 + 2\frac{\dot{a}}{a}\frac{\dot{b}}{b} = 8\pi G(\rho^I + \rho^A), \quad (2.10)$$

$$\frac{\ddot{a}}{a} + \frac{\ddot{b}}{b} + \frac{\dot{a}}{a}\frac{\dot{b}}{b} = -8\pi G(p^I + p_\parallel^A), \quad (2.11)$$

$$2\frac{\ddot{a}}{a} + \left(\frac{\dot{a}}{a}\right)^2 = -8\pi G(p^I + p_\perp^A). \quad (2.12)$$

In the following we shall restrict our analysis to the case of matter-dominated universe ($p^I = 0$) filled with an anisotropic component given by a uniform magnetic field (directed along the z -axis), or a cosmic domain wall (whose plane of symmetry is the xy -plane), or a cosmic string (directed along the z -axis).

Magnetic fields have been observed on a wide range of scales. In particular, they have been detected in galaxies, galaxy clusters, and also in extra-galactic structures (for recent reviews on cosmic magnetic fields, see Ref. [13]). It is reasonable to assume that the actual observed magnetic fields have a primordial origin. We assume that a (almost) uniform magnetic field pervades our universe, though it is not excluded that such a field may have a more complicated structure on small scales.

Further examples of anisotropic components are given by cosmic topological defects [20]. As it is well known, phase transitions in the early universe can generate domain walls (cosmic strings), which are two-dimensional (one-dimensional) defects that originate when a discrete (axial or cylindrical) symmetry is broken.

For the three cases discussed above, the energy-momentum tensor take on the form

$$(T_B)^\mu{}_\nu = \rho_B \text{diag}(1, -1, -1, 1), \quad (2.13)$$

$$(T_w)^\mu{}_\nu = \rho_w \text{diag}(1, 1, 1, 0), \quad (2.14)$$

$$(T_s)^\mu{}_\nu = \rho_s \text{diag}(1, 0, 0, 1), \quad (2.15)$$

where ρ_B , ρ_w , and ρ_s , are the magnetic, wall, and string energy density, respectively. Moreover, we assume that the interaction of anisotropic components with matter is negligible (in the case of magnetic fields, this corresponds to taking into account that the conductivity of the primordial plasma is very high [13]). In this case, the

anisotropic component of the energy-momentum tensor is conserved, $(T_A)^\mu_{\nu;\mu} = 0$, so that we have

$$\dot{\rho}^A + 2\frac{\dot{a}}{a}(\rho^A + p_{\parallel}^A) + \frac{\dot{b}}{b}(\rho^A + p_{\perp}^A) = 0. \quad (2.16)$$

Let us introduce the eccentricity

$$e = \sqrt{1 - \left(\frac{b}{a}\right)^2}, \quad \text{or} \quad e = \sqrt{1 - \left(\frac{a}{b}\right)^2}, \quad (2.17)$$

and normalize the scale factors such that $a(t_0) = b(t_0) = 1$ at the present time t_0 . The first definition of eccentricity applies to the cases of uniform magnetic field or string, while the second one to the case of domain wall.

In this paper, we restrict our analysis to the case of small eccentricities (that is we consider the metric anisotropies as perturbations over the isotropic Friedmann-Robertson-Walker background). In this limit, from Eqs. (2.10)-(2.12), we get the following evolution equation for the eccentricity:

$$\frac{d(e\dot{e})}{dt} + 3H(e\dot{e}) = \pm 8\pi G(p_{\parallel}^A - p_{\perp}^A), \quad (2.18)$$

where the plus sign refers to the cases of magnetic field and string, while the minus sign to the case of domain wall. Here $H = \dot{a}/a$ is the usual Hubble expansion parameter for the isotropic universe. In the matter-dominated era, it results $a(t) \propto t^{2/3}$, so that $H = 2/(3t)$.

Moreover, to the zero-order in the eccentricity, from Eq. (2.16) it follows that the energy densities (and pressure) scale in time as $\rho_B \propto a^{-4}$, $\rho_w \propto a^{-1}$, and $\rho_s \propto a^{-2}$, for the three cases, respectively.

The solution of Eq. (2.18) for the magnetic case is

$$e^2 = 8\Omega_B^{(0)}(1 - 3a^{-1} + 2a^{-3/2}), \quad (2.19)$$

where $\Omega_B^{(0)} = \rho_B(t_0)/\rho_{\text{cr}}^{(0)}$, and $\rho_{\text{cr}}^{(0)} = 3H_0^2/8\pi G$ is the actual critical energy density. At the decoupling, $t = t_{\text{dec}}$, we have $e_{\text{dec}}^2 \simeq 16\Omega_B^{(0)}z_{\text{dec}}^{3/2}$, where $e_{\text{dec}} = e(t_{\text{dec}})$ and $z_{\text{dec}} \simeq 1088$ is the red-shift at decoupling [4]. Accordingly, we get:

$$e_{\text{dec}} \simeq 10^{-2} \left(\frac{\Omega_B^{(0)}}{10^{-7}} \right)^{1/2}, \quad (2.20)$$

or

$$e_{\text{dec}} \simeq 10^{-2} h^{-1} \frac{B_0}{10^{-8} \text{G}}, \quad (2.21)$$

where $B_0 = B(t_0)$ and $h \simeq 0.72$ [4] is the little- h constant.

If, for instance, we assume for the present cosmological magnetic field strength the estimate $B_0 \simeq 5 \times 10^{-9} \text{G}$, which is compatible with the constraints analyzed in Ref. [21], we get an eccentricity at decoupling of order $e_{\text{dec}} \sim 10^{-2}$.

In the cases of domain wall and cosmic string, integrating Eq. (2.18), we find

$$e^2 = \frac{2}{7} \Omega_w^{(0)} (3a^2 + 4a^{-3/2} - 7) \quad (2.22)$$

and

$$e^2 = \frac{4}{5} \Omega_s^{(0)} (3a + 2a^{-3/2} - 5), \quad (2.23)$$

respectively, where $\Omega_w^{(0)}$ and $\Omega_s^{(0)}$ are the actual energy densities, in units of $\rho_{\text{cr}}^{(0)}$, associated to domain wall and cosmic string.

From the above equations, we can estimate the eccentricity at decoupling in terms of wall and string energy densities at present time:

$$e_{\text{dec}} \simeq 10^{-2} \left(\frac{\Omega_w^{(0)}}{5 \times 10^{-7}} \right)^{1/2}, \quad (2.24)$$

and

$$e_{\text{dec}} \simeq 10^{-2} \left(\frac{\Omega_s^{(0)}}{4 \times 10^{-7}} \right)^{1/2}. \quad (2.25)$$

Vice versa, since the analysis of the CMB radiation constrains the value of the eccentricity at decoupling to be less than 10^{-2} (see Ref. [10] and next Section), one gets an upper limit on the values of the energy density of cosmic defects stretching our universe of order $\Omega_{w,s}^{(0)} \lesssim 10^{-7}$.

3 CMB Quadrupole Anisotropy

Let us begin by briefly discussing the standard analysis of the CMB temperature anisotropies [22]. First, the temperature anisotropy is expanded in terms of spherical harmonics:

$$\frac{\Delta T(\theta, \phi)}{\langle T \rangle} = \sum_{l=1}^{\infty} \sum_{m=-l}^l a_{lm} Y_{lm}(\theta, \phi). \quad (3.1)$$

After that, one introduces the power spectrum:

$$\frac{\Delta T_l}{\langle T \rangle} = \sqrt{\frac{1}{2\pi} \frac{l(l+1)}{2l+1} \sum_m |a_{lm}|^2}, \quad (3.2)$$

that fully characterizes the properties of the CMB anisotropy. In particular, the quadrupole anisotropy refers to the multipole $\ell = 2$:

$$\mathcal{Q} \equiv \frac{\Delta T_2}{\langle T \rangle}, \quad (3.3)$$

where $\langle T \rangle \simeq 2.73\text{K}$ is the actual (average) temperature of the CMB radiation. The quadrupole problem resides in the fact that the observed quadrupole anisotropy is in the range (see Table 1):

$$(\Delta T_2)_{\text{obs}}^2 \simeq (210 \div 276) \mu\text{K}^2, \quad (3.4)$$

while the expected quadrupole anisotropy according the Λ CDM standard model is:

$$(\Delta T_2)_I^2 \simeq 1252 \mu\text{K}^2. \quad (3.5)$$

If we admit that the large scale spatial geometry of our universe is plane-symmetric with a small eccentricity, then we have that the observed CMB anisotropy map is a linear superposition of two contributions [10, 23]:

$$\Delta T = \Delta T_A + \Delta T_I, \quad (3.6)$$

where ΔT_A represents the temperature fluctuations due to the anisotropic space-time background, while ΔT_I is the standard isotropic fluctuation caused by the inflation-produced gravitational potential at the last scattering surface. As a consequence, we may write:

$$a_{lm} = a_{lm}^A + a_{lm}^I. \quad (3.7)$$

We are interested in the distortion of the CMB radiation in a universe with planar symmetry described by the metric (2.1). As before, we will work in the small eccentricity approximation. From the null geodesic equation, we get that a photon emitted at the last scattering surface having energy E_{dec} reaches the observer with an energy equal to $E_0(\hat{n}) = \langle E_0 \rangle (1 - e_{\text{dec}}^2 n_3^2/2)$, where $\langle E_0 \rangle \equiv E_{\text{dec}}/(1 + z_{\text{dec}})$, and $\hat{n} = (n_1, n_2, n_3)$ are the direction cosines of the null geodesic in the symmetric (Robertson-Walker) metric.

It is worth mentioning that the above result applies to the case of the axis of symmetry directed along the z -axis. We may, however, easily generalize this result to the case where the symmetry axis is directed along an arbitrary direction in a coordinate system (x_g, y_g, z_g) in which the $x_g y_g$ -plane is, indeed, the galactic plane. To this end, we perform a rotation $\mathcal{R} = \mathcal{R}_x(\vartheta) \mathcal{R}_z(\varphi + \pi/2)$ of the coordinate system (x, y, z) , where $\mathcal{R}_z(\varphi + \pi/2)$ and $\mathcal{R}_x(\vartheta)$ are rotations of angles $\varphi + \pi/2$ and ϑ about the z - and x -axis, respectively. In the new coordinate system the magnetic field is directed along the direction defined by the polar angles (ϑ, φ) . Therefore, the temperature anisotropy in this new reference system is:

$$\frac{\Delta T_A}{\langle T \rangle} \equiv \frac{E_0(n_A) - \langle E_0 \rangle}{\langle E_0 \rangle} = -\frac{1}{2} e_{\text{dec}}^2 n_A^2, \quad (3.8)$$

where $n_A \equiv (\mathcal{R} \hat{n})_3$ is equal to

$$n_A(\theta, \phi) = \cos \theta \cos \vartheta - \sin \theta \sin \vartheta \cos(\phi - \varphi). \quad (3.9)$$

Alternatively, when the eccentricity is small, Eq. (2.1) may be written in a more standard form:

$$ds^2 = dt^2 - a^2(t)(\delta_{ij} + h_{ij}) dx^i dx^j, \quad (3.10)$$

where h_{ij} is the metric perturbation which takes on the form:

$$h_{ij} = -e^2 \delta_{i3} \delta_{j3}. \quad (3.11)$$

The null geodesic equation in a perturbed Friedmann-Robertson-Walker metric gives the temperature anisotropy (Sachs-Wolfe effect):

$$\frac{\Delta T}{\langle T \rangle} = -\frac{1}{2} \int_{t_{\text{dec}}}^{t_0} dt \frac{\partial h_{ij}}{\partial t} n^i n^j, \quad (3.12)$$

where n^i are the directional cosines. Using $e(t_0) = 0$, from Eqs. (3.11) and (3.12) one gets:

$$\frac{\Delta T}{\langle T \rangle} = -\frac{1}{2} e_{\text{dec}}^2 n_3^2, \quad (3.13)$$

which indeed agrees with our previous result.

It is easy to see from Eq. (3.8) that only the quadrupole terms ($\ell = 2$) are different from zero:

$$\begin{aligned} a_{20}^{\text{A}} &= -\frac{\sqrt{\pi}}{6\sqrt{5}} [1 + 3 \cos(2\vartheta)] e_{\text{dec}}^2, \\ a_{21}^{\text{A}} &= -(a_{2,-1}^{\text{A}})^* = \sqrt{\frac{\pi}{30}} e^{-i\varphi} \sin(2\vartheta) e_{\text{dec}}^2, \\ a_{22}^{\text{A}} &= (a_{2,-2}^{\text{A}})^* = -\sqrt{\frac{\pi}{30}} e^{-2i\varphi} \sin^2 \vartheta e_{\text{dec}}^2. \end{aligned} \quad (3.14)$$

Consequently, the quadrupole anisotropy is:

$$\mathcal{Q}_{\text{A}} = \frac{2}{5\sqrt{3}} e_{\text{dec}}^2. \quad (3.15)$$

Since the temperature anisotropy is a real function, we have $a_{l,-m} = (-1)^m (a_{l,m})^*$. Observing that $a_{l,-m}^{\text{A}} = (-1)^m (a_{l,m}^{\text{A}})^*$ [see Eq. (3.14)], we get $a_{l,-m}^{\text{I}} = (-1)^m (a_{l,m}^{\text{I}})^*$. Moreover, because the standard inflation-produced temperature fluctuations are statistically isotropic, we will make the reasonable assumption that the a_{2m}^{I} coefficients are equals up to a phase factor. Therefore, we can write:

$$\begin{aligned} a_{20}^{\text{I}} &= \sqrt{\frac{\pi}{3}} e^{i\phi_1} \mathcal{Q}_{\text{I}}, \\ a_{21}^{\text{I}} &= -(a_{2,-1}^{\text{I}})^* = \sqrt{\frac{\pi}{3}} e^{i\phi_2} \mathcal{Q}_{\text{I}}, \\ a_{22}^{\text{I}} &= (a_{2,-2}^{\text{I}})^* = \sqrt{\frac{\pi}{3}} e^{i\phi_3} \mathcal{Q}_{\text{I}}, \end{aligned} \quad (3.16)$$

where $0 \leq \phi_i \leq 2\pi$ are unknown phases, and

$$\mathcal{Q}_{\text{I}} \simeq 13 \times 10^{-6}. \quad (3.17)$$

Taking into account Eqs. (3.14) and (3.16), and Eqs. (3.1), (3.2) and (3.7), we get for the total quadrupole:

$$\mathcal{Q}^2 = \mathcal{Q}_{\text{A}}^2 + \mathcal{Q}_{\text{I}}^2 - 2f \mathcal{Q}_{\text{A}} \mathcal{Q}_{\text{I}}, \quad (3.18)$$

Table 1: The cleaned maps SILC400, WILC3YR, and TCM3YR. Note that the values of a_{2m} in this table correspond to the values of a_{2m} given in Refs. [24, 5, 25] divided by $\langle T \rangle \simeq 2.73K$. The values of the angles ϕ_2 , and ϕ_3 are in degrees.

MAP	m	$\text{Re}[a_{2m}]/10^{-6}$	$\text{Im}[a_{2m}]/10^{-6}$	ϕ_2	ϕ_3	$(\Delta T_2)^2/\mu\text{K}^2$
SILC400	0	2.75	0.00	107.6	44.2	275.8
	1	-0.56	1.77			
	2	-6.79	-6.60			
WILC3YR	0	4.21	0.00	90.6	52.5	248.8
	1	-0.02	1.78			
	2	-5.28	-6.89			
TCM3YR	0	1.22	0.00	86.8	49.2	209.5
	1	0.10	1.79			
	2	-5.45	-6.32			

where

$$\begin{aligned}
f(\vartheta, \varphi; \phi_1, \phi_2, \phi_3) &= \frac{1}{4\sqrt{5}} \{2\sqrt{6} [\sin \vartheta \cos(2\varphi + \phi_3) - 2 \cos \vartheta \cos(\varphi + \phi_2)] \sin \vartheta \\
&+ [1 + 3 \cos(2\vartheta)] \cos \phi_1\}.
\end{aligned} \tag{3.19}$$

Looking at Eq. (3.18) we see that, if the space-time background is not isotropic, the quadrupole anisotropy can become smaller than the one expected in the standard picture of the Λ CDM (isotropic-) cosmological model of temperature fluctuations. We may fix the direction of the magnetic field and the eccentricity by solving Eq. (3.7), which is (for $\ell = 2$) a system of 5 equations containing 5 unknown parameters: e_{dec} , ϑ , φ , ϕ_2 , and ϕ_3 . Note that it is always possible to choose a_{20} real, and then $\phi_1 = 0$.

To solve Eq. (3.7) for $\ell = 2$, we need the observed values of the a_{2m} 's. We use the recent cleaned CMB temperature fluctuation map of the WMAP3 data obtained by using an improved internal linear combination method as Galactic foreground subtraction technique. In particular, we adopt the three maps SILC400 [24], WILC3YR [5], and TCM3YR [25]. For completeness, we report in Table 1 the values of a_{2m} corresponding to these maps. We also indicate the values of ϕ_2 and ϕ_3 [found by solving Eq. (3.16)] in the case of isotropic universe ($a_{2m}^{\text{A}} = 0$). Moreover, for sake of definiteness, we assume that the planar symmetry is induced by a cosmological magnetic field with strength B_0 at the present time.

Numerical solutions of Eq. (3.7), referring to the three maps, are given in Tables 2, 3, and 4, respectively. In the Appendix, we will show that the system (3.7) admits at most 8 independent solutions. However, due to the particular values taken by the a_{2m} for the three different maps, we find that to the map SILC400 it corresponds 8 independent solutions, while to the maps WILC3YR and TCM3YR there correspond only 4 independent solutions.

Moreover we observe that, for each independent solution ($e_{\text{dec}}, \vartheta, \varphi, \phi_2, \phi_3$) shown in

Table 2: Numerical solutions of Eq. (3.7) obtained by using the map SILC400; the values of the angles ϑ , φ , ϕ_2 , and ϕ_3 are in degrees.

$e_{\text{dec}}/10^{-2}$	ϑ	φ	ϕ_2	ϕ_3	$B_0/10^{-9}\text{G}$
0.69	38.6	80.1	100.8	34.8	5.0
0.69	38.4	99.2	83.7	20.9	4.9
0.68	38.3	37.2	139.1	66.8	4.9
0.67	37.4	139.3	47.3	12.8	4.8
0.63	35.3	308.9	43.2	17.3	4.5
0.62	34.5	281.2	73.6	25.8	4.5
0.62	34.3	239.8	122.5	48.9	4.4
0.62	34.3	255.2	104.2	39.9	4.4

Table 3: Numerical solutions of Eq. (3.7) obtained by using the map WILC3YR; the values of the angles ϑ , φ , ϕ_2 , and ϕ_3 are in degrees.

$e_{\text{dec}}/10^{-2}$	ϑ	φ	ϕ_2	ϕ_3	$B_0/10^{-9}\text{G}$
0.69	40.6	91.7	88.6	28.0	4.9
0.69	40.6	88.3	91.6	30.8	4.9
0.67	40.0	139.4	45.6	8.6	4.8
0.67	40.0	40.4	134.6	71.0	4.8

Table 4: Numerical solutions of Eq. (3.7) obtained by using the map TCM3YR; the values of the angles ϑ , φ , ϕ_2 , and ϕ_3 are in degrees.

$e_{\text{dec}}/10^{-2}$	ϑ	φ	ϕ_2	ϕ_3	$B_0/10^{-9}\text{G}$
0.70	36.5	96.6	83.8	24.9	5.0
0.70	36.5	83.2	95.7	35.1	5.0
0.69	36.1	129.4	54.3	9.4	5.0
0.69	36.0	51.6	124.1	59.8	5.0

the tables, there exists another one given by $(e_{\text{dec}}, \pi - \vartheta, \varphi \pm \pi, \phi_2, \phi_3)$, where we take the plus sign if $\varphi < \pi$ and the minus sign if $\varphi > \pi$.

Looking at Table 1 and Eq. (3.17), we see that the values of coefficients $|a_{21}|$ are about one order of magnitude smaller than \mathcal{Q}_I . Assuming $\mathcal{Q}_I \gg |a_{21}|$, we will show in the Appendix that an approximate solution for e_{dec} and ϑ is:

$$e_{\text{dec}}^2 \simeq \sqrt{10} \mathcal{Q}_I, \quad (3.20)$$

and

$$\vartheta \simeq \frac{1}{2} \arccos \left[\frac{(5\sqrt{5} - \sqrt{6\pi})\mathcal{Q}_I - 5\sqrt{3}a_{20}}{3\sqrt{6\pi}\mathcal{Q}_I} \right]. \quad (3.21)$$

From Eq. (3.20) we also have that $e_{\text{dec}} \simeq 0.64 \times 10^{-2}$, $B_0 \simeq 4.6 \times 10^{-9}\text{G}$, and $\mathcal{Q}_A \simeq (4/\sqrt{30})\mathcal{Q}_I \simeq 0.7\mathcal{Q}_I$. From Eq. (3.21) we get, for the three different maps, $\vartheta \simeq 34^\circ, 36^\circ, 31^\circ$, respectively. As one can easily check, the approximate solutions Eqs. (3.20) and (3.21) are quite close to the numerical values.

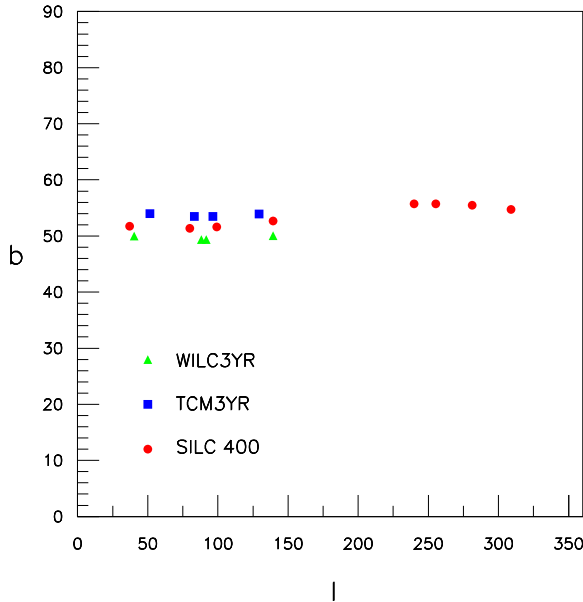


Figure 1: Numerical solutions of Eq. (3.7) obtained by using the three maps. Note that $b = 90^\circ - \vartheta$, and $l = \varphi$, where (b, l) are the galactic coordinates.

In Fig. 1, we plot the numerical solutions ϑ versus φ (which define the direction of the symmetry axis), using the so-called galactic coordinates system characterized by the galactic latitude b , and galactic longitude l . In our notation, the angle b corresponds to $b = 90^\circ - \vartheta$ while $l = \varphi$. From Fig. 1 we see that the galactic latitude

of the symmetry axis is remarkably independent on the adopted CMB temperature fluctuation map. On the contrary, we find that the galactic longitude is poorly constrained, for it may vary in a large interval. Indeed, we have $b \simeq 50^\circ - 54^\circ$, while $40^\circ \lesssim l \lesssim 140^\circ$, $240^\circ \lesssim l \lesssim 310^\circ$. One could think of choosing the value of φ (for each map) by imposing that the corresponding solution $(e_{\text{dec}}, \vartheta, \varphi, \phi_2, \phi_3)$ has the smallest difference between (ϕ_2, ϕ_3) and those in absence of anisotropic component listed in Table 1. Since such a difference indicates how much the intrinsic quadrupole needs to be rotated to accommodate the anisotropic component, the above choice would represent the “least radical modification” to the standard (isotropic) cosmological model. For the three maps SILC400, WILC3YR, TCM3YR, we could then pick the solutions corresponding to $l = \varphi \simeq 255^\circ, 88^\circ, 83^\circ$, respectively. Also in this case, however, we cannot univocally fix the galactic longitude of the magnetic field.

It is interesting to stress that our determination of the direction of the symmetry axis is in fair agreement with the statistical analysis of Ref. [24] which confirmed the strong alignment and planarity of the quadrupole and the octupole. Thus, we see that our proposal for an ellipsoidal universe could provide a natural solution to the low- ℓ CMB puzzles.

4 Limits on Cosmic Magnetic Fields from Big Bang Nucleosynthesis and Large Scale Structure formation.

In the previous Section, we have seen that ellipsoidal universe with an eccentricity at decoupling $e_{\text{dec}} \simeq 0.64 \times 10^{-2}$ could provide a natural solution to the low quadrupole CMB puzzle. We believe that the most interesting and intriguing possibility is plane-symmetric geometry induced by cosmological magnetic fields. In fact, magnetic fields are observed in the universe up to cosmological scales. So that, we cannot exclude that the origin of the presently-observed cosmic magnetic fields is primordial as long the predictions of the standard cosmological model are not invalidate. Indeed, our estimate for the present-time magnetic field strength,

$$B_0 \simeq 4.6 \times 10^{-9} \text{ G}, \quad (4.1)$$

is in agreement with the observed magnetic fields within galaxies and clusters of galaxy [13]. However, the presence of a cosmic primordial magnetic field must also fulfil the constraints coming from Big Bang Nucleosynthesis (BBN) and Large Scale Structure (LSS) formation.

Limits from BBN. Since in the early universe the conductivity of the primordial plasma is very high, magnetic fields are frozen into the plasma and evolve adiabatically, $B \propto a^{-2}$, where $a \propto g_{*S}^{-1/3} T^{-1}$, T being the temperature, and g_{*S} counts the total number of effectively massless degrees of freedom referring to the entropy density of the universe [26].

The limit coming from BBN refers to uniform magnetic fields at that time. The upper bound is given in Ref. [27]:

$$B(T_{\text{BBN}}) \lesssim 1 \times 10^{11} \text{ G}, \quad (4.2)$$

where $T_{\text{BBN}} = 10^9 \text{K} \simeq 0.1 \text{MeV}$. This limit translates into:

$$B_0 = \left(\frac{g_{*S}(T_0)}{g_{*S}(T_{\text{BBN}})} \right)^{2/3} \left(\frac{T_0}{T_{\text{BBN}}} \right)^2 B(T_{\text{BBN}}) \lesssim 6 \times 10^{-7} \text{G}, \quad (4.3)$$

where $B_0 = B(T_0)$, and we used $g_{*S}(T_{\text{BBN}}) \simeq g_{*S}(T_0) \simeq 3.91$, and $T_0 \simeq 2.35 \times 10^{-4} \text{eV}$ [26]. We see, indeed, that our estimate (4.1) does not violate the upper bound (4.3).

Limits from LSS. Anisotropic cosmological models have been extensively studied since long time (see, for instance, Ref. [28] and references therein). It is known that strong anisotropic expansion could influence the formation of large-scale structures. In particular, in case of strong anisotropies in the expansion of the universe the time of growth of structures could increase by a factor 3 – 5 [28].

In matter-dominated universe, we see from Eq. (2.19) that the eccentricity evolves as $e^2(z) \propto z^{3/2}$. So that, at the epoch of matter-radiation equality we get:

$$e_{\text{eq}} \simeq \left(\frac{z_{\text{eq}}}{z_{\text{dec}}} \right)^{3/2} e_{\text{dec}} \simeq 5.5 e_{\text{dec}} \simeq 3.5 \times 10^{-2}, \quad (4.4)$$

where $e_{\text{eq}} = e(z_{\text{eq}})$ and we used $z_{\text{dec}} \simeq 1088$, $z_{\text{eq}} \simeq 3400$ [26], and $e_{\text{dec}} \simeq 0.64 \times 10^{-2}$. Thus, we see that at the epoch of matter-radiation equality the anisotropy in the cosmological expansion is small. So that, we do not expect dramatic effects on the processes of growth of structures. Nevertheless, it could well be that small anisotropies in the cosmic expansion could leave signatures on large scales which should be contrasted with observations.

5 Conclusions

The recent measurements of the cosmic microwave background angular spectrum have greatly improved our understanding of the universe, in particular we have information on the properties and origin of the density fluctuation of the cosmic plasma. In fact, the observed CMB fluctuations are in remarkable agreement with the prediction of the ΛCDM standard model with scale-invariant adiabatic fluctuations generated during the inflationary epoch. However, some anomalies have been discovered on large angular scales including, in particular, the low CMB quadrupole power and the alignment and planarity of the quadrupole and octupole modes. It should be stressed, however, that the large-angle anomalies in the CMB anisotropy are still subject to an intense debate [29]. For instance, it has been suggested that the CMB anomalies could be explained by the residual Galactic foreground emission [30]. Therefore, it is very important to improve and develop techniques which allow a better removal of residual foreground contamination [31].

In this paper, we have further elaborated our previous proposal [10] that an “ellipsoidal expansion” of the universe could resolve the CMB quadrupole anomaly. We have shown that such anisotropic expansion (described by a plane-symmetric metric) can be generated by cosmological magnetic fields or topological defects, such as cosmic domain walls or cosmic strings. Indeed, topological cosmic defects are relic

structures that are predicted to be produced in the course of symmetry breaking in the hot, early universe. Nevertheless, we believe that the most interesting and intriguing possibility is plane-symmetric geometry induced by cosmological magnetic fields. In fact, magnetic fields have been already observed in the universe up to cosmological scales.

We have shown that the quadrupole anomaly can be resolved if the last scattering surface of CMB is an ellipsoid. Indeed, we found that, if the eccentricity at decoupling is:

$$e_{\text{dec}} \simeq 0.64 \times 10^{-2}, \quad (5.1)$$

then the quadrupole amplitude can be drastically reduced without affecting higher multipoles of the angular power spectrum of the temperature anisotropy. Remarkably, our estimate of e_{dec} gives for the strength of the cosmic magnetic field:

$$B_0 \simeq 4.6 \times 10^{-9} \text{ G}, \quad (5.2)$$

which agrees with the limits arising from primordial nucleosynthesis and large scale structure formation. Moreover, we have obtained tight constraints on the direction (b, l) of the axis of symmetry:

$$b \simeq 50^\circ - 54^\circ, \quad 40^\circ \lesssim l \lesssim 140^\circ, \quad 240^\circ \lesssim l \lesssim 310^\circ, \quad (5.3)$$

where b and l are the galactic latitude and the galactic longitude, respectively. This constraints are in fair agreement with recent statistical analyses of the cleaned CMB temperature fluctuation maps of the WMAP3 data obtained by using an improved internal linear combination method as Galactic foreground subtraction technique.

In conclusion, our proposal for the ellipsoidal universe offers a natural solution to the CMB quadrupole anomaly which future pattern searches with more refined data, such as further WMAP data releases or PLANK data, will be able to confirm or reject. In addition, recently it has been shown [32] that the large scale polarization of the cosmic microwave background induced by an ellipsoidal universe compares quite well to the average level of polarization detected by the Wilkinson Microwave Anisotropy Probe. Still, it is necessary to better understand the foreground contamination of the polarization to reach a firm conclusion.

Finally, we find amusing that there are already independent indications of a symmetry axis in the large-scale geometry of the universe, coming from the analysis of spiral galaxies in the Sloan Digital Sky Survey [33] and the analysis of polarization of electromagnetic radiation propagating over cosmological distances [34].

6 Appendix

In this Appendix, we solve the system of equations (3.7) for $\ell = 2$. The numerical values of the a_{2m} 's are listed in Table 1, while the a_{2m}^A 's and a_{2m}^I 's are given by Eq. (3.14) and Eq. (3.16), respectively.

Since it is always possible to choose a_{20} real, we take $\phi_1 = 0$. Moreover, the temperature anisotropy is real so that we have $a_{2,-m} = (-1)^m (a_{2m})^*$, $a_{2,-m}^A = (-1)^m (a_{2m}^A)^*$, and $a_{2,-m}^I = (-1)^m (a_{2m}^I)^*$. Therefore, the system of equations (3.7) reduces to:

$$a_{20} = -\frac{\sqrt{\pi}}{6\sqrt{5}} [1 + 3 \cos(2\vartheta)] e_{\text{dec}}^2 + \sqrt{\frac{\pi}{3}} \mathcal{Q}_I, \quad (6.1)$$

$$\text{Re}[a_{21}] = \sqrt{\frac{\pi}{30}} \cos\varphi \sin(2\vartheta) e_{\text{dec}}^2 + \sqrt{\frac{\pi}{3}} \cos\phi_2 \mathcal{Q}_I, \quad (6.2)$$

$$\text{Im}[a_{21}] = -\sqrt{\frac{\pi}{30}} \sin\varphi \sin(2\vartheta) e_{\text{dec}}^2 + \sqrt{\frac{\pi}{3}} \sin\phi_2 \mathcal{Q}_I, \quad (6.3)$$

$$\text{Re}[a_{22}] = -\sqrt{\frac{\pi}{30}} \cos\varphi \sin^2\vartheta e_{\text{dec}}^2 + \sqrt{\frac{\pi}{3}} \cos\phi_3 \mathcal{Q}_I, \quad (6.4)$$

$$\text{Im}[a_{22}] = \sqrt{\frac{\pi}{30}} \sin\varphi \sin^2\vartheta e_{\text{dec}}^2 + \sqrt{\frac{\pi}{3}} \sin\phi_3 \mathcal{Q}_I, \quad (6.5)$$

where \mathcal{Q}_I is given by Eq. (3.17). We see that these equations form a system of 5 transcendental equations containing 5 unknown parameters: e_{dec} , ϑ , φ , ϕ_2 , and ϕ_3 . Solving Eq. (6.1) with respect to ϑ we get two independent solutions:

$$\vartheta = \{\tilde{\vartheta}, \pi - \tilde{\vartheta}\}, \quad (6.6)$$

where

$$\tilde{\vartheta} = \frac{1}{2} \arccos\left(\frac{5\sqrt{5\pi}\mathcal{Q}_I - 5\sqrt{15}a_{20} - \sqrt{3\pi}e_{\text{dec}}^2}{3\sqrt{3\pi}e_{\text{dec}}^2}\right). \quad (6.7)$$

Squaring Eqs. (6.4) and (6.5), adding side by side, and then solving with respect to φ , we obtain 8 independent solutions:

$$\varphi = \{\tilde{\varphi}_{\pm}, \pi - \tilde{\varphi}_{\pm}, 2\pi - \tilde{\varphi}_{\pm}, \pi + \tilde{\varphi}_{\pm}\}, \quad (6.8)$$

where

$$\tilde{\varphi}_{\pm} = \frac{1}{2} \arccos\left(\frac{\alpha\gamma \pm \beta\sqrt{\alpha^2 + \beta^2 - \gamma^2}}{\alpha^2 + \beta^2}\right), \quad (6.9)$$

and

$$\alpha = \sqrt{\frac{2\pi}{15}} \text{Re}[a_{22}] \sin^2\vartheta e_{\text{dec}}^2, \quad (6.10)$$

$$\beta = \sqrt{\frac{2\pi}{15}} \text{Im}[a_{22}] \sin^2\vartheta e_{\text{dec}}^2, \quad (6.11)$$

$$\gamma = \frac{\pi}{30} \sin^4\vartheta e_{\text{dec}}^4 + |a_{22}|^2 - \frac{\pi}{3} \mathcal{Q}_I^2. \quad (6.12)$$

By dividing side by side Eqs. (6.3) and (6.2), and solving with respect to ϕ_2 , we get:

$$\tan\phi_2 = \frac{\sqrt{30} \operatorname{Im}[a_{21}] + \sqrt{\pi} \sin\varphi \sin(2\vartheta) e_{\text{dec}}^2}{\sqrt{30} \operatorname{Re}[a_{21}] - \sqrt{\pi} \sin\varphi \sin(2\vartheta) e_{\text{dec}}^2}. \quad (6.13)$$

The same procedure applied to Eqs. (6.5) and (6.3) results in:

$$\tan\phi_3 = \frac{\sqrt{30} \operatorname{Im}[a_{22}] - \sqrt{\pi} \sin(2\varphi) \sin^2\vartheta e_{\text{dec}}^2}{\sqrt{30} \operatorname{Re}[a_{22}] + \sqrt{\pi} \sin(2\varphi) \sin^2\vartheta e_{\text{dec}}^2}. \quad (6.14)$$

Finally, by squaring Eqs. (6.2) and (6.3), and adding side by side, we get:

$$e_{\text{dec}}^4 + 2c e_{\text{dec}}^2 - d = 0, \quad (6.15)$$

where we have defined

$$c(\varphi, \vartheta) = \sqrt{\frac{30}{\pi}} (\operatorname{Re}[a_{21}] \cos\varphi - \operatorname{Im}[a_{21}] \sin\varphi) \csc(2\vartheta), \quad (6.16)$$

$$d(\varphi, \vartheta) = 10 \left(\mathcal{Q}_I^2 - \frac{3}{\pi} |a_{21}|^2 \right) \csc^2(2\vartheta). \quad (6.17)$$

We observe that the couple (ϑ, φ) can assume 16 different values, according to Eqs. (6.6) and (6.8). Inserting these values in Eqs. (6.15)-(6.17) we arrive at 16 different equations for e_{dec} . It is straightforward to verify that only 8 of these are “independent”, in the sense that, given a solution $(e_{\text{dec}}, \vartheta, \varphi)$ of one of the “independent” equations, then $(e_{\text{dec}}, \pi - \vartheta, \varphi \pm \pi)$ is a solutions of one of the “dependent” ones (we must take the plus sign if $\varphi < \pi$ and the minus sign if $\varphi > \pi$). The 8 independent equations can be solved numerically and their solutions are presented in Table 2, 3, and 4. Here, we just observe that, to the map SILC400 it corresponds 8 independent solutions, while to the maps WILC3YR and TCM3YR there correspond only 4 independent solutions.

Finally, we derive the approximate solutions (3.20)-(3.21). To this end, we may formally solve Eq. (6.15) to get $e_{\text{dec}}^2 = c \pm \sqrt{c^2 + d}$. If $\mathcal{Q}_I \gg |a_{21}|$ then $d \gg c^2$, and we obtain $e_{\text{dec}}^2 \simeq \sqrt{10} \mathcal{Q}_I |\csc(2\vartheta)|$. Now, it is easy to check numerically that $|\csc(2\vartheta)| \simeq 1$. Indeed, from Table 2, 3, 4, we get $1.01 \lesssim |\csc(2\vartheta)| \lesssim 1.07$. As a consequence, we have $e_{\text{dec}}^2 \simeq \sqrt{10} \mathcal{Q}_I$, which indeed agrees with Eq. (3.20). Inserting Eq. (3.20) into Eq. (6.7) we easily recover Eq. (3.21).

References

- [1] G. F. Smoot *et al.*, *Astrophys. J.* **396**, L1 (1992); C. L. Bennett *et al.*, *ibid.* **464**, L1 (1996).
- [2] <http://wmap.gsfc.nasa.gov/>
- [3] D. N. Spergel *et al.*, *Astrophys. J. Suppl.* **170**, 377 (2007); L. Page *et al.*, *ibid.*, 335 (2007); C. L. Bennett *et al.*, *ibid.* **148**, 1 (2003); G. Hinshaw *et al.*, *ibid.* **148**, 135 (2003).
- [4] D. N. Spergel *et al.*, *ibid.* **148**, 175 (2003).
- [5] G. Hinshaw *et al.*, *ibid.* **170**, 288 (2007).
- [6] N. J. Cornish *et al.*, *Phys. Rev. Lett.* **92**, 201302 (2004); B. F. Roukema *et al.*, *Astron. Astrophys.* **423**, 821 (2004); T. R. Jaffe *et al.*, *Astrophys. J.* **629**, L1 (2005); [astro-ph/0606046](#); J. G. Cresswell *et al.*, *Phys. Rev. D* **73**, 041302 (2006); T. Ghosh, A. Hajian and T. Souradeep, *ibid.* **75**, 083007 (2007).
- [7] G. Efstathiou, *Mon. Not. Roy. Astron. Soc.* **343**, L95 (2003); B. Feng and X. Zhang, *Phys. Lett. B* **570**, 145 (2003); M. Kawasaki and F. Takahashi, *ibid.* **570**, 151 (2003); S. Tsujikawa, R. Maartens, and R. Brandenberger, *ibid.* **574**, 141 (2003); J. M. Cline, P. Crotty and J. Lesgourgues, *JCAP* **0309**, 010 (2003); C. R. Contaldi *et al.*, *ibid.* **0307**, 002 (2003); S. DeDeo, R. R. Caldwell and P. J. Steinhardt, *Phys. Rev. D* **67**, 103509 (2003) [Erratum-*ibid.* **D 69**, 129902 (2004)].
- [8] C. Gordon and W. Hu, *Phys. Rev. D* **70**, 083003 (2004); T. Moroi and T. Takahashi, *Phys. Rev. Lett.* **92**, 091301 (2004); J. Weeks *et al.*, *Mon. Not. Roy. Astron. Soc.* **352**, 258 (2004); Y. S. Piao, *Phys. Rev. D* **71**, 087301 (2005); D. Boyanovsky, H. J. de Vega and N. G. Sanchez, *Phys. Rev. D* **74**, 123006 (2006); *ibid.* **74**, 123007 (2006); C. H. Wu *et al.*, *JCAP* **0702**, 006 (2007); M. Demianski and A. G. Doroshkevich, [arXiv:astro-ph/0702381](#); J. Beltran Jimenez and A. L. Maroto, [arXiv:astro-ph/0703483](#).
- [9] A. de Oliveira-Costa *et al.*, *Phys. Rev. D* **69**, 063516 (2004); D. J. Schwarz *et al.*, *Phys. Rev. Lett.* **93**, 221301 (2004); K. Land and J. Magueijo, *ibid.* **95**, 071301 (2005); C. J. Copi *et al.*, *Mon. Not. Roy. Astron. Soc.* **367**, 79 (2006); L. R. Abramo *et al.*, *Phys. Rev. D* **74**, 063506 (2006); L. R. Abramo, L. Sodre Jr. and C. A. Wuensche, *ibid.* **74**, 083515 (2006); Y. Wiaux *et al.*, *Phys. Rev. Lett.* **96**, 151303 (2006); L. Ackerman, S. M. Carroll and M. B. Wise, *Phys. Rev. D* **75**, 083502 (2007); P. Vielva *et al.*, [arXiv:0704.3736 \[astro-ph\]](#); A. Pontzen and A. Challinor, [arXiv:0706.2075 \[astro-ph\]](#).
- [10] L. Campanelli, P. Cea and L. Tedesco, *Phys. Rev. Lett.* **97**, 131302 (2006) [Erratum-*ibid.* **97**, 209903 (2006)].
- [11] X. H. Ge and S. P. Kim, [arXiv:hep-th/0703117](#).

- [12] A. Berera, R. V. Buniy, and T. W. Kephart, JCAP **0410**, 016 (2004);
R. V. Buniy, A. Berera, and T. W. Kephart, Phys. Rev. D **73**, 063529 (2006).
- [13] D. Grasso and H. R. Rubinstein, Phys. Rept. **348**, 163 (2001); L. M. Widrow,
Rev. Mod. Phys. **74**, 775 (2003); M. Giovannini, Int. J. Mod. Phys. D **13**, 391
(2004).
- [14] J. D. Barrow, R. Maartens and C. G. Tsagas, arXiv:astro-ph/0611537.
- [15] D. R. Matravers and C. G. Tsagas, Phys. Rev. D **62**, 103519 (2000);
C. G. Tsagas, Phys. Rev. Lett. **86**, 5421 (2001); F. de Felice, F. Sorge and
S. Zilio, Class. Quant. Grav. **22**, 47 (2005).
- [16] For generation mechanisms of cosmic magnetic fields during inflation see, e.g.:
M. S. Turner and L. M. Widrow, Phys. Rev. D **37**, 2743 (1988); B. Ratra,
Astrophys. J. **391**, L1 (1992); A. Dolgov, Phys. Rev. D **48**, 2499 (1993);
D. Lemoine and M. Lemoine, *ibid.* **52**, 1955 (1995); M. Gasperini, M. Gio-
vannini and G. Veneziano, Phys. Rev. Lett. **75**, 3796 (1995); K. Dimopoulos
et al., *ibid.* **65**, 063505 (2002); M. M. Anber and L. Sorbo, JCAP **0610**, 018
(2006).
- [17] For general properties of inflation-produced magnetic fields see: C. G. Tsagas,
Phys. Rev. D **72**, 123509 (2005); K. Bamba and M. Sasaki, JCAP **0702**, 030
(2007).
- [18] For generation mechanisms of cosmic magnetic fields after inflation see, e.g.:
G. Sigl, A. V. Olinto, and K. Jedamzik, Phys. Rev. D **55**, 4582 (1997); P. Cea
and L. Tedesco, Phys. Lett. B **450**, 61 (1999); T. Vachaspati, Phys. Rev. Lett.
87, 251302 (2001); V. I. Demchik and V. V. Skalozub, Eur. Phys. J. C **25**,
291 (2002); Z. Berezhiani and A. D. Dolgov, Astropart. Phys. **21**, 59 (2004);
V. B. Semikoz and D. D. Sokoloff, Phys. Rev. Lett. **92**, 131301 (2004); M. Laine,
JHEP **0510**, 056 (2005).
- [19] A. H. Taub, Annals Math. **53**, 472 (1951).
- [20] T. W. B. Kibble, J. Phys. **A9**, 1387 (1976); Phys. Rept. **67**, 183 (1980);
A. Vilenkin and E. P. S. Shellard, *Cosmic Strings and Other Topological Defects*
(Cambridge University Press, Cambridge, England, 1994).
- [21] J. D. Barrow, P. G. Ferreira and J. Silk, Phys. Rev. Lett. **78**, 3610 (1997).
- [22] S. Dodelson, *Modern Cosmology* (Academic Press, San Diego, California, 2003).
- [23] E. F. Bunn, P. Ferreira, and J. Silk, Phys. Rev. Lett. **77**, 2883 (1996).
- [24] C. G. Park, C. Park, and J. R. I. Gott, Astrophys. J. **660**, 959 (2007).
- [25] A. de Oliveira-Costa and M. Tegmark, Phys. Rev. D **74**, 023005 (2006).

- [26] E. W. Kolb and M. S. Turner, *The Early Universe* (Addison-Wesley, Redwood City, California, 1990).
- [27] D. Grasso and H. R. Rubinstein, Phys. Lett. B **379**, 73 (1996).
- [28] Y. B. Zeldovich and I. D. Novikov, *Relativistic Astrophysics. Vol. 2: The Structure and Evolution of the Universe* (University of Chicago Press, Chicago, Illinois, 1983).
- [29] E. Gaztanaga *et al.*, Mon. Not. Roy. Astron. Soc. **346**, 47 (2003); G. Efstathiou, *ibid.* **346**, L26 (2003); *ibid.* **348**, 885 (2004); I. J. O'Dwyer *et al.*, Astrophys. J. **617**, L99 (2004); A. Rakic and D. J. Schwarz, Phys. Rev. D **75**, 103002 (2007).
- [30] A. Rakic, S. Rasanen and D. J. Schwarz, Mon. Not. Roy. Astron. Soc. **369**, L27 (2006); arXiv:astro-ph/0609188, *Talk given at 11th Marcel Grossmann Meeting on Recent Developments in Theoretical and Experimental General Relativity, Gravitation, and Relativistic Field Theories, Berlin, Germany, 23-29 Jul 2006*.
- [31] W. N. Brandt *et al.*, Astrophys. J. **424**, 1 (1994); M. Tegmark and G. Efstathiou, Mon. Not. Roy. Astron. Soc. **281**, 1297 (1996); C. Bennett *et al.*, Astrophys. J. Suppl. **148**, 97 (2003); C. G. Park, C. Park and J. R. I. Gott, Astrophys. J. **660**, 959 (2007).
- [32] P. Cea, arXiv:astro-ph/0702293.
- [33] M. J. Longo, arXiv:astro-ph/0703325; arXiv:astro-ph/0703694.
- [34] B. Nodlang and J. P. Ralston, Phys. Rev. Lett. **78**, 3043 (1997); D. Hutsemekers *et al.*, Astron. Astrophys. **441**, 915 (2005).